Systematics, functional morphology and distribution of a bivalve (*Apachecorbula muriatica gen. et sp. nov.*) from the "shores" of the "Valdivia Deep" brine pool in the Red Sea

P. Graham Oliver[1], Hege Vestheim[2], André Antunes[3] & Stein Kaartvedt[2]

[1]National Museum of Wales, Cathays Pk., Cardiff, Wales, UK, CF10 3NP e-mail graham.oliver@museumwales.ac.uk
[2] King Abdullah University of Science and Technology, Red Sea Research Center, Thuwal, 23955-6900, Saudi Arabia
[3] IBB-Institute for Biotechnology and Bioengineering, Centre of Biological Engineering, Micoteca da Universidade do Minho, University of Minho, Braga, Portugal

ABSTRACT

The deep brine pools of the Red Sea comprise extreme, inhospitable habitats, yet housing microbial communities which potentially may fuel adjacent fauna. We here describe a novel bivalve at a deep–sea (1525 m) brine pool in the Red Sea, where conditions of high salinity, lowered pH, partial anoxia and high water temperatures are prevalent. ROV footage showed that the clams were present in a narrow (20 cm) band along the "shores" of the brine, suggesting that the clam is not only tolerant of the extreme conditions but is also limited to them. The clam is attributed to the family Corbulidae and named as Apachecorbula muriatica gen et sp nov. *The shell morphology is atypical of the family in being modioliform in outline and very thin. The semi-infaunal habit is seen in ROV images and is reflected in the anatomy by the lack of siphons. The ctenidium is large and typical of a suspension feeding bivalve, but the absence of "guard cilia" and the greatly reduced palps suggest that it is not selective and this is a response to low food availability. It is proposed that the low body mass observed is a consequence of the the extreme conditions and low food availability, yet higher than in the adjacent deep sea. It is postulated that the observed morphology of* Apachecorbula *is a result of paedomorphosis driven by the effects of the extreme environment on growth but is in part mitigated by the absence of high predation pressures.*

Keywords: Corbulidae, deep-hyper-saline anoxic basins (DHABs), Red Sea, Deep-sea, Apachecorbula gen. nov., Functional morphology, Valdivia Deep, Deep sea clams

INTRODUCTION

Deep-sea anoxic brine pools are formed by the solution of evaporate deposits and the stable accumulation of these hypersaline solutions in enclosed depressions on the sea floor (Bischoff 1969, Hartmann 1985). They are known from the Gulf of Mexico (Cordes et al. 2010), eastern Mediterranean and are widespread in the Red Sea with 25 known to date (Atunes et al., 2011). The brine pools are both highly saline and usually anoxic in addition to having a high metal content and low pH but harbour a unique microbial community of extremophiles (Antunes et al, 2011). Metazoans are absent from the extremes of anoxia but in the Red Sea have been recorded from the shores of a shallow and less saline site (Thuwal Seeps) (Batang et al, 2012) as well as along the Kebrit brine pool (Vestheim & Kaartvedt, *in prep*.). Bivalve mollusks including a species of Corbuloidea, were recorded from the Thuwal Seeps but have not been studied beyond a tentative identification (*Corbula cf. rotalis*) due to lack of samples. The presence of bacterial mats at the Thuwal deep suggest that this is an active cold seep site. The Kebrit brine shore hosted solemyid clams which are obligate chemosymbiotic and one live individual of a corbulid were also found (Vestheim & Kaartvedt, *in prep*.). In the Gulf of Mexico dense beds of the chemosymbiotic *Bathymodiolus childressi* (Gustafson et al., 1998) are found around the margins of a cold seep brine pool (MacDonald et al. 1990). In the eastern Mediterranean meiofaunal communities have been found in hypersaline sediments with sparse macrofauna at the margins. Juvenile bivalves were found in the meiofaunal samples but were not identified (Lampadariou et al., 2003).

In April 2013 the Valdivia Deep brine pool, situated in the central Red Sea (21° 20′ 49″N, 37° 57′ 19″E) (Fig. 1) at a depth of 1525 metres was investigated by an expedition from the King Abdullah University of Science and Technology. Video footage from a ROV revealed small, black bivalves along the shores of the brine pool. Bivalves were sampled for further analyses together with analyses of environmental conditions, and

turned out to be a novel species and genera of clams. The Valdivia clams are living in conditions of high salinity, low oxygen, lowered pH and relatively high temperatures. This paper addresses their identity and systematic relationships and explores their functional morphology in relation to the extreme environmental conditions in which they are found.

MATERIALS AND METHODS

Data were collected in April 2013, using the RV Aegaeo (4th King Abdullah University of Science and Technology (KAUST) Red Sea Expedition.

Environment

Data on temperature, pH, salintiy and oxygen were collected using a specially designed CTD, able to withstand the corrosive brine environment. The instrument package also included probes for measuring oxygen and pH.

Underwater observation, collection and preservation

Underwater observations were conducted using the ROV Max Rover (DSSI, USA) system as described in Batang et al. (2012) and Vestheim & Kaartvedt (*in prep*.). Sediment samples were collected using the ROV's robotic arm fitted with a fabric bag. The samples were then transferred to the surface in the bag and immediately inspected in the lab. Individual clams were picked out and either frozen in N_2(l) or preserved in ethanol (70%), glutaraldehyde (EM grade) or 4% buffered formaldehyde solution, as further outlined in the Result & Discussion section. Preserved samples were stored at 4^{o}C upon analysis.

No live macrofauna exept for the corbulid clams were found in the sediments. The sediment mainly consisted of biogenic material being remains of shelled pelagic snails (pteropods) and some calcified foraminiferans along with mineral particles.

Morphology

Morphology was examined by gross dissection following staining of tissues in Haematoxylin. Scanning electron microscopy of tissues followed dehydration in 100% ethanol and critical point drying, gold coating and microscopy with a Jeol Neoscope; shell micrographs were taken on a FEI Quanta 200 or Jeol Neoscope. Shells were examined without cleaning and following cleaning with dilute bleach. The terminology associated with hinge structures follows that of Anderson & Roopnarine (2003). The shell measuments are shown in Fig. 4.

Molecular data and analysis

In order to confirm the family placement and ascertain affinities within the Corbulidae a molecular analysis was carried out. Total genomic DNA was extracted from ten ethanol preserved specimens using the DNA Easy Blood and Tissue Kit (Qiagen) following the manufacture's protocol for animal tissue. DNA yield of the extractions was quantified on a Qubit 2.0 fluorometer (invitrogen) and partial COI, 28S, 18S and 16S sequences were generated by PCR using the primer pairs as described in Table 1. The 25 µL PCR reactions included 5 µL 5X Phusion buffer, 0.5 µL 10 mM dNTPs, 1.25 µL each primer (10 µM), 1.25 µL 50 mM MgCl, 0.125 µL Phusion High-Fidelity DNA polymerase and 1µL DNA extract (~10 ng/µL).Thermal cycling conditions were: 98^{o}C for 2 min, then 37 cycles of 98^{o}C for 30 s, 30-40 s at annealing temperature (see Table 1) and 72^{o}C for 1 min, followed by a final extension 10 min at 72^{o}C. A negative (no template DNA) and positive control (template DNA known to amplify) were included in all PCRs. All PCR products were checked on a 1% agarose gel and cleaned with illustra ExoStar 1-Step (GE Healthcare) before sequenced on an ABI 3730xl Capillary Sequencer (Applied Biosystems) using the respectively forward and backward PCR primer.

Table 1. List of PCR primers used in this study.

Primer pair	Target	Annealing temperature	Reference
LCO1490/HCO2198	COI	50^{o}C	Folmer et al., 1994
16Sa/16Sb	16S	50^{o}C	Xiong & Kocher, 1991

3F/18sbi, 1F/5R, 18Sa2.0/9R	18S	48ºC	Giribet et al., 1996; Whiting et al., 1997
C1/C4	28S	52ºC	Lorion et al., 2010

Contiguous sequences were after manually inspection compared with other corbulid sequences. No other, appropriately preserved, corbulids from the Red Sea were available for molecular analysis and all comparisons were made from previously published DNA sequences available through GenBank and from Anders Hallan (Hallan et al., 2013). There was only one 16S (*Corbula tunicata* KC429314, partial sequence, not overlapping) and no COI sequences from closely related corbulids available for comparison at the time of analysis, hence phylogentic analysis for those genes were not performed. For 28S and 18S sequences phylogenetic analysis was executed on the Phylogeny.fr platform (Dereeper et al., 2008) using a MUSCLE alignment (Edgar, 2004), GBLOCKS curation of the nucleotide alignment allowing gaps in the final alignment (Castresana, 2000), the PhyML phylogeny package (Guindin & Gascuel, 2003) and the HKY85 nucleotide substitution model with approximate likelihood-ratio test for branch support (Anisimova & Gascuel 2006). Tree rendering was performed with TreeDyn (Chevenet et al. 2006).

RESULTS AND DISCUSSION

Environmental conditions

Vertical profiles of temperature, salinity, dissolved oxygen and pH were almost constant with depth until close proximity to the surface of the brine pool. Within a five metre zone the water quality parameters change rapidly and significantly (Fig.2, Table 2). At 1525 metres the salinity is 53 but within a further two metres depth it has risen to 220. Similar rapid changes in environmental parameters over this two metre range are seen in dissolved oxygen dropping from 2.9 mg/l to 0.9 mg/l; ph dropping from 7.8 to 6.5 while water temperature rises from 23.4°C to 26.1°C.

Table 2. CTD data for a depth range of 1525-1530 m indicating rapid and significant changes in salinity, dissolved oxygen, pH and temperature.

Water Depth (m)	Temperature (°C)	pH	Salinity	Oxygen (mg l^{-1})
1525.2	23.4	7.8	53	2.9
1526.0	23.9	7.1	82	2.4
1526.6	24.7	6.8	205	1.0
1527.2	25.5	6.7	219	0.9
1527.9	26.0	6.7	217	0.9
1528.7	26.6	6.6	222	0.8
1529.4	27.8	6.5	226	0.8
1530.2	28.7	6.5	231	0.7

Video footage

Video footage from the ROV revealed a barren fringe around the brine pool except for small black clams living half buried in the sediment (Fig. 3A-C). The band of clams could be seen stretching into the distance in Fig. 3C. The ROV footage showed that the clams were present in a narrow (20 cm) band along the shores of the Valdivia deep. The clams seemed to sit on the hill tops, not in the valleys (topographic depressions) suggesting that they are responding closely to changes in water chemistry. Counting one site (frame) gave an estimate of 130 individuals within 70x20 cm, though the distribution was patchy. This high density corresponds to approximately 900 individuals m^{-2}. The distribution within a narrow band suggests that the clam is not only tolerant of the extreme conditions but is also limited to them. This is unlike *Bathymodiolus childressi* which tolerates hypersalinity but is not restricted to such environments (Carney et al. 2006).

No other live metazoans were observed in the sediments collected with the clams, which therefore seem quite unique in inhabiting the Valdivia shore sediment. There was further no evidence of a chemosynthetic community such as seen at the Thuwal Seeps (Batang et al., 2012) or at the Kebrit brine pool (Vestheim & Kaartvedt*, in prep*.). This is in keeping with the lack of hydrothermal activity at the Valdivia Deep as demonstrated by Zierenberg & Shanks (1986).

171 One individual of the same species of clam were also found along the Kebrit brine pool
172 (Vestheim & Kaartvedt, *in prep*.).
173
174 **Phylogentics**
175 There was no intraspecific variation among the clam indiviuals sequenced.
176 Representative contiguous sequences have been deposited to EMBL database under the
177 accession numbers HG942537 (COI), HG942542 (16S), HG942541 (18S) and
178 HG942543 (28S). Based on comparison of 18S and 28S partial sequences (data not
179 shown), the Valdivia clam fits within the "Western pacific group" of Hallan et al. (2013)
180 that includes *Caryocorbula coxi* Pilsbry,1897 and *Caryocorbula*? *zelandica* Quoy &
181 Gaimard,1835, '*Corbula sinensis*' Bernard, Cai & Morton, 1993, *Notocorbula hydropica*
182 as well as 'Notocorbula coxi' (AY192684, misidentified in GenBank (Hallan et al. 2013))
183 and *Corbula gibba* Olivi, 1792. The sequences available were not informative enough to
184 conclude anything more on the phylogentic relationship to these species.
185
186 TAXONOMY

187 SYSTEMATICS

188 Bivalvia Linnaeus, 1758

189 Heterodonta Neumayr, 1884

190 Order Myoida Stoliczka, 1870

191 Superfamily Myoidea Lamarck, 1809

192 Family Corbulidae Lamarck, 1818

193 Genus ***Apachecorbula*** Oliver & Vestheim, gen. nov.

194 Type species: *A. muriatica* Oliver, this paper, monotypic

195 **Definition**

Small, thin, translucent shelled, slightly inequivalve, strongly inequilateral, prosogyre beaks close to the anterior. Outline obliquely oval, modioliform. Hinge weak, right valve with a single anterior cardinal and a thin posterior flange; left valve with a cardinal complex of a cardinal socket, median projecting chondrophore and a small projecting knob behind the chondrophore; a narrow posterior flange also present.

Etymology

From the Greek apaches meaning "without thickness" (Brown, 1956); referring to the thin shell and insubstantial soft tissues.

Comparisons

There are few systematic studies of the Corbulidae but that of Anderson & Roopnarine (2003) lists forty genera of which fourteen are extant and of these only seven have an Indo-Pacific distribution. A very recent study by Hallan et al. (2013) presented the most comprehensive molecular based study to date and indicated that, for the marine genera included, the clades corresponded poorly with shell based genera. However, in general the marine Corbulidae have thick shells and are distinctly inequivalve. Two main shell forms are exhibited: (1) inflated, trigonal, posterior narrowly rostrate (2) subovate, posterior narrow, subtruncate. In the Red Sea the former is represented by *Corbula* (*Varicorbula*) *erythraeenisis* Adams, 1871 and the latter by *Corbula* (*Anisocorbula*) sulculosa Adams, 1870. The thin, slightly inequivalve and modioliform shell is not seen in any of the described genera. The molecular study confirmed the placement within the Corbulidae and showed that *Apachecorbula* has closer affinity with other Indo- Pacific genera than those from the Western Atlantic/Caribbean. This distinction between the corbulids of the two regions was first noted by Anderson & Roopnarine (2003) and reiterated by Hallan et al. (2013).

Apachecorbula muriatica Oliver & Vestheim, gen. et sp. nov.

Material examined

40 specimens, Valdivia Brine Pool, Red Sea, 21° 20 49 N, 37° 57 19 E, 1525 m. R/V Aegaeo, 2013 KAUST Red Sea Expedition, 12/iv/2013.

Holotype, 1 specimen, as above. NMW.Z. 2013.058.1

Paratypes, 10 specimens as holotype, NMW.Z.2013.058.2; remaining specimens as holotype KAUST.

1 specimen, Kebrit Brine Pool, Red Sea, 24°43 00N, 36° 16 00E, 1465 m. R/V Aegaeo, 2013 KAUST Red Sea Expedition, 15/iv/2013.

Comparative material examined

Corbula (Varicorbula) sp.1. 8 shells, Central Red Sea, RV "Valdivia" station 741GKW, 24°43.100 N 36°15.500 E, 1465m. 08/03/1981. Senckenberg-Museum

Corbula (Varicorbula) erythraeensis. 20 shells, Gulf of Suez, Red Sea, ex Macandrew, National Museum of Wales, Melvill-Tomlin Coll. NMW.1955.158. 4 spec. Ras Budran Oilfield, Gulf of Suez, 28°57 N 33°10 E, ex Oil Pollution Rsearch Unit/ JP Hartley, 1980-83, NMWZ. 1982.068.

Corbula (Anisocorbula) sulculosa. 20+ specimens, Ras Budran Oilfield, Gulf of Suez, 28°57 N 33°10 E, ex Oil Pollution Rsearch Unit/ JP Hartley, 1980-83, NMWZ. 1982.068.

Corbula (Anisocorbula) taitensis 2 shells, Masirah, Oman, Arabian Sea, 20°12 N 58°42 E, NMWZ 1993.61.1282.

Corbula (Varicorbula) rotalis. 10 shells, Hizen, Japan, Melvill-Tomlin Coll. NMW.1955.158.

Corbua (Varicorbula) gibba [Type species of *Varicorbula*]. Many specimens in collection of NMW from locations around the British Isles. Juveniles from the Irish Sea, NMWZ.2005.015.

Corbula sulcata [Type species of *Corbula*] 3 shells, Senegal, West Africa, ex Caziot, Melvill-Tomlin Coll. NMW.1955.158.

Corbula (Anisocorbula) macgillivrayi [Type species of *Anisocorbula*] 1 shell, Australia, Melvill-Tomlin Coll. NMW.1955.158.

Table 3. *Apachecorbula muriatica* sp. nov. Measurements (mm).

	Preservation	L (rv)	L (lv)	H (rv)	H (lv)	T (rv)	T (lv)	Total T	AL
1A	100% Eth	6.2	5.9	5	4.8	1.6	1.5	3.2	1.7
1B	100% Eth	6	5.7	4.7	4.4	2	1.1	3.1	1.5
1C	100% Eth	5.7	5.3	4.6	4.2	1.8	1.3	3.1	1.2
1D	100% Eth	5.4	4.9	4.6	4	2	1.6	3.6	1.4
1E	100% Eth	5.6	5.3	5.4	5.7	bk	bk	bk	1.6
2A	Form to 80% Eth	4.9	4.7	3.8	3.6	1.6	1	2.6	1.3
2B	Form to 80% Eth	4.9	4.6	4	3.7	1.5	1.2	2.7	1.2
2C	Form to 80% Eth	bk	bk	bk	bk	bk	bk	bk	bk
2D	Form to 80% Eth	5.7	5.4	4.7	4.5	bk	bk	bk	1.3
2E	Form to 80% Eth	4.6	4.4	3.8	3.5	1.3	1.2	2.5	1
3A	Form to 80% Eth	5.4	5.1	4.4	4	1.8	1.4	3.2	1
3B	Form to 80% Eth	4.7	4.4	3.8	3.5	1.5	1.1	2.6	1
3C	Form to 80% Eth	5.3	5.2	4.4	4.3	1.7	1.3	3	1.2
3D	Form to 80% Eth	5.6	5.2	4.5	4.1	1.5	1.2	2.7	1.2
3E	Form to 80% Eth	5.3	5	4.2	3.7	1.8	1.2	3	1
4A	Form to 80% Eth	5.1	4.8	4.2	3.9	1.7	1.6	3.3	1.2
4B	Form to 80% Eth	5	4.7	4.1	3.6	1.6	1	2.7	1.3
4C	Form to 80% Eth	5.1	4.8	4	3.4	1.5	1.2	2.7	0.9
4D	Glut to 80%Eth	6.1	5.7	4.7	4.3	1.6	1.5	3.1	1.4
4E	Glut to 80%Eth	5.6	5.2	4.3	3.7	1.7	1.4	3.1	1.3
5A	Glut to 80%Eth	5.4	5.1	4.3	3.7	1.9	1.2	3.1	1.4
5B	Glut to 80%Eth	4	3.9	3.2	2.8	1.2	1	2.2	0.9
5C	Glut to 80%Eth	5.6	5.3	4.2	3.8	1.8	1.3	3.1	1.2
5D	Glut to 80%Eth	4.6	4.2	4.1	3.6	1.5	1.1	2.6	1.1
5E	Glut to 80%Eth	5.2	4.8	4.1	3.5	1.6	1.3	2.9	1.1
6A	Glut to 80%Eth	5.5	5.2	4.2	3.5	1.8	1.3	3.1	1.1
6B	Glut to 80%Eth	4.3	4.1	3.5	3.2	1.4	1.3	2.7	0.9
6C	Glut to 80%Eth	4.2	4.1	3.4	3.1	1.3	1	2.3	0.8
6D	Glut to 80%Eth	4.4	4.1	3.6	3.2	1.5	1.1	2.6	0.9
6E	Glut to 80%Eth	5.2	4.9	4.3	3.8	1.6	1.4	3	1.5
7A	Glut to 80%Eth	4.8	4.5	3.9	3.5	1.6	1.3	2.9	1.2
7B	Glut to 80%Eth	4.1	3.9	3.6	3.1	1.3	0.8	2.1	0.8

7C	Glut to 80%Eth	4.4	4.2	3.7	3.2	1.6	1	2.6	1.1
7D	Glut to 80%Eth	bk	bk	bk	bk	bk	bk	bk	bk
7E	Glut to 80%Eth	bk	bk	bk	bk	bk	bk	bk	bk
8A	Glut to 80%Eth	bk	bk	bk	bk	bk	bk	bk	bk
HOLOTYPE	DRY	5.8	5.6	4.7	4.4	ds	ds	ds	1.4
SEM	DRY GOLD	9.2	8.7	6.9	6.2	ds	ds	ds	1.6

Description – Shell Figs (5-7)

To 9 mm in length. Typical shell as represented by the holotype (Fig. 5) very thin approximately 16µm in cross section (Fig. 7A), translucent, fragile. Inequivalve, left valve the slightly smaller, slightly less inflated fitting inside the larger right valve. Outline inequilateral, prosogyrous beaks in the anterior fifth. Outline obliquely oval, modioliform, anterior narrowly rounded, posterior expanded, subtruncate. Umbonal – posterior ventral angle distinct but low, more strongly expressed in the right valve. Hinge weak, LV (Fig. 6A,B) with a cardinal complex of a median narrow chondrophore (ch), posterior to it a small projecting knob (kn), anterior to it a socket for the cardinal tooth in the RV (c sk). RV (Fig. 6C) with a small cardinal peg-like tooth (c th) widely separated from an elongate, thin, submarginal posterior, weakly serrated, flange (Fig. 6D), Internal ligament attached to chondrophore and sub-umbonal gap, external ligament short, thin (Fig. 6A, B, ext lig):

Sculpture weak, without magnification smooth with weak incremental lines except for the margins of the RV of larger specimens where commarginal ridges develop and are best seen with SEM (Fig. 6G). Under the SEM both valves with radial and commarginal creasing of the periostracum (Fig. 6E), this reflected only very lightly as shell sculpture (Fig. 6H, circled). LV with increasing lamellar periostracum at the margins with sparse radial creases (Fig. 6F). Indications of shell spines on the dorsal margin of the RV (Fig. 6I, arrowed).

Shell colourless with sparse, black deposits. Deposits composed of aggregated spherules, with a compact reticulate surface (Fig. 7B, C).

Variation

The shape of the shell is occasionally variable. Some shells are far less inequilateral and have a more rounded appearance (Fig. 5G) while some although strongly inequilateral have a more rounded posterior outline (Fig. 5E). This variability can be expressed in the "length : height" ratio of the right valves while there is a mean of 1.23 and a range from 1.04 – 1.33. The inequilateral condition expressed as the ratio "length : anterior length" has a mean of 4.47 and a range from 3.47 to 5.67. The extent of the inequivalve condition is also variable, while the mean ratio for right and left valve tumidity is 1.33 the range is from 1.06 to 1.82.

Description – Anatomy Figs 7-8

The mantle edge is thin (Fig. 8B) and largely fused except for an anterior pedal aperture Fig. 8A, pg) and small posterior inhalant and exhalant apertures (Fig. 8A, ex, in). The musculature of the posterior apertures is weak and siphons are not developed (Fig. 8C). The inner edge of the inhalant aperture bears minute widely spaced pointed papillae and a few papillae are also present on the outer edges (Fig. 8C). The exhalant aperture has a few papillae on the outer edge but the inner edge is smooth (Fig. 8C). The adductor muscles are small (Fig. 8A) and the pedal protractor muscles are very thin.

The volume of the shell is filled with the large ctenidium composed of two demibranchs with reflexed filaments, the outer demibranch is approximately two-thirds the size of the inner (Figs 8A, B). The filaments (Figs 9A-D) are narrow with heavily ciliated frontal surfaces (Fig. 9A) and are inter-connected with regularly spaced muscular junctions best seen from the abfrontal face (Fig. 9B). The frontal ciliation (Fig. 9D) is composed of a row of frontal cilia (fc) bounded on either side by a row of lateral frontal cirri (lfc), these bounded by a row of lateral cilia (lc) that lie slightly to the posterior and are seen from the abfrontal surface. The frontal cilia give way to longer terminal cilia (tc) towards the food groove. The lateral frontal cirri appear as lamellar structures with multiple fine ends

(Fig. 9C) and arise from prominent ridged bases (lfc[b]), this in contrast with the frontal and terminal cilia that arise from a punctate cushion-like surface (tc[b]).

Labial palps are vestigial and lack sorting ridges.

The foot and visceral mass are proportionately small compared to the mantle cavity and are contained within the anterior dorsal region (Fig. 8A). The foot (Fig. 8D, f) has a long toe and a short heel these separated by a small byssal groove. The byssus is active and produces a very fine thread that has a multiple split end (Fig. 8A, by).

The alimentary system (Figs 8A, D, E) is composed of a short oesophagus (oe), a stomach (st) with two distinct parts, a dorsal cavity and a ventral tube housing the style sac (ss). The digestive diverticula (dg) are confined to the immediate surrounds of the stomach and open by a single ventral aperture into the stomach. The remainder of the gut and rectum are not coiled.

A small portion of gonadal tissue (Fig. 8E, gd) was observed but the detailed structure and that of the heart and kidneys could not be discerned by gross dissection.

Etymology

From the Latin *muriaticus* meaning “of brine” (Brown, 1956); referring to the brine pool habitat.

Comparisons

Only three identified species of Corbulidae are recorded from the Red Sea, *C. (Varicorbula) erythraeensis* Adams, 1871 (Fig. 10A-B), *C. (Ansiocorbula) sulculosa* Adams, 1870 (Fig. 10D-E) and *C. (A.) taitensis* Lamarck, 1818 (Fig. 10G-H) (Oliver, 1990). Unidentified species of *Corbula* were listed by Grill & Zuschin (2001) and a further but undescribed species has been collected from the deep central Red Sea and is referred to here as *C. (Varicorbula)* sp. 1 (Fig. 11A-D, 12F-I). A fifth was recorded from the Thuwal Seep and tentatively identified as *C. (V.) rotalis* (Batang et al, 2012), shells from the type locality of Japan are illustrated here (Fig. 10C & F). Both species of

Anisocorbula have almost equilateral heavy strongly sculptured shells quite unlike *Apachecorbula*. The other three species can be assigned to the subgenus *Varicorbula* and have inequilateral, strongly inequivalve, robust shells with a prominent commarginal sculpture on the right valve. These characters contrast with the thin and modioliform shell of *Apachecorbula*. As stated under the generic remarks *Apachecorbula* is unlike all other corbulid genera in the weakly inequivalve, modioliform and thin shell but these are characters seen in the juvenile shells of some species. Juvenile *Anisocorbula* are distinctly carinate and some have a pustulose microsculpture (Fig 12C-D), both characters not seen in *Apachecorbula*. Juveniles of *Varicorbula* are quadrate in outline (Fig. 12A) with the anterior narrower than the posterior, with growth they become narrow, almost rostrate, posteriorly. These juveniles have a distinct umbonal angulation and are almost carinate in some, the left valve has a wide non calcified margin and is weakly pustulose in *C. (V.) erythraeensis* (Fig. 12A-B); this in contrast with the shell of *A. muriaticus*. In *Varicorbula* sp. 1 the ribbed sculpture of the right valve appears at an early stage, approxiately at one millimetre (Fig. 12G) and has no radial sculptural element on the early shell (Fig. 12F). The indications of dorsal spines in *Apachecorbula* are reminiscent of the distinct spines present in juvenile of the European *C. (V.) gibba* (Fig. 12E). Given the differences outlined here and the relatively large size of *Apachecorbula* we conclude that this does not represent a juvenile of any known species. The presence of gonadal tissue also suggests that these specimens are adult.

DISCUSSION on FUNCTIONAL MORPHOLOGY

The footage from the ROV (Fig. 3) shows that *Apachecorbula* is semi-infaunal with only the anterior part of the shell within the sediment. Despite the slender nature of the byssus it is a constant feature and will help to stabilize this position. This life habit with the posterior part of the shell well above the sediment surface may account for the absence of well developed siphons in *Apachecorbula* and is in contrast with the siphonate condition found in all other corbulids studied (Yonge 1946, Morton 1990, Mikkelsen & Bieler 2001). Shallow water corbulids are generally described as shallow burrowers with the

posterior part of the shell lying at or close to the sediment surface (Yonge 1946, Morton 1990). Yonge (1946) makes reference to the heavy sediment load experienced by *C. (V.) gibba* and relates this to the form and function of the papillate siphons and the large quantities of pseudofaeces produced. Mikkelsen & Bieler (2001) record instances of *C. (V.) disparilis* being epifaunal but with no fixed position, rather living among shell hash. The morphology of *C. (V.) disparilis* is essentially similar to other shallow water species and has well developed papillate siphons. The paucity of siphonal papillae in *Apachecorbula* may be related to the semi-infaunal habit but may also reflect the potential paucity of suspended food particles available to it.

The large gill, its ciliation and lack of gut coiling suggest that *Apachecorbula* is a suspension feeder. Deep-sea deposit feeding bivalves typically have coiled mid and hind guts, and large labial palps or palp probosides (Allen, 1979). There is no abfrontal extension indicative of forms harbouring chemosymbiotic bacteria (Taylor & Glover, 2010) and no bacteriocyte cells were observed. The diversity of suspension feeding bivalves in the deep sea is limited primarily to Arcidae and Limopsidae (Oliver, 1979) and for the relatively well studied Atlantic deep-sea fauna corbulids are all but absent from the bathyal and abyssal zones (Allen, 2008). As a suspension feeder *Apachecorbula* might be expected to have labial palps at least as large as other species in the family but this is not so as the palps are very small. This suggests that sorting of food particles is reduced and this is supported by the absence of guard cilia on the food groove of the ctenidium. Yonge (1946) suggested that the guard cilia in *C. (V.) gibba* functioned to prevent unwanted non-food particles being carried to the labial palps and mouth. Their absence, reduced palps and weak papillation of the inhalant aperture all suggest that *Apachecorbula* is not subjected to a large load of suspended particles entering the mantle cavity and does not sort particles to the same extent as shallow water species. Together this suggests that food is in short supply.

The overall appearance of the soft tissues is one of contracted size and lack of substance except for the ctenidia. We propose that the large ctenidium is maintained to facilitate

386 both food collection and respiration in conditions of low food and low oxygen. However,
387 these adaptations do not overcome the severe conditions and the body mass is relatively
388 small compared to the volume of the shell thus reducing the metabolic demand. A similar
389 low body mass was reported in *Amygdalum anoxicolum,* a glassy mussel from the oxygen
390 minimum zone off Oman (Oliver, 2001).

391

392 A number of studies on corbulids note the thick shell and presence of conchioloin layers
393 Yonge (1946) on *C. (V.) gibba* from Scotland; Morton (1990) on *C. crassa* from Hong
394 Kong and Mikkelsen & Bieler (2001) on *C. (V.) disparilis* from Florida. The conchiolin
395 layers are postulated to prevent predation by shell-boring gastropods, their absence in *A.*
396 *muriaticus* suggests that such predation pressures do not exist. The thin shell reduces the
397 energy demand for shell production especially in an environment that is slightly acidic.

398

399 It has been noted above that the shell of *Apachecorbula* most resembles that of the
400 juvenile shells of *Varicorbula* suggesting that paedomorphosis has occurred. The shells
401 are relatively large (9 mm) compared with species that have evolved by progenesis, e.g.
402 *Turtonia minuta* at 2 mm (Ockelmann, 1964) and *Notolimea clandestina* at 1mm (Salas,
403 1994). Hayami and Kase (1993) cited abnormal salinity, metallic cat-ions (Fe, Cu),
404 oxygen deficiency, high turbidity, strong water agitation, high population density,
405 abnormal pH, temperature variations and deficient food supply as possible causes of
406 stunting. Many of these factors apply to the extreme environment of the "shore" of the
407 brine pool yet the size is not atypically small in comparison with other Red Sea corbulids
408 that have a maximum size of 13 mm in *Varicorbula sp. 1* and *Anisocorbula taitensis.* The
409 feeble musculature, small size of the visceral mass and small adductor muscles do
410 however give an impression of stunting such that there is "a small body in a large shell"
411 appearance to *Apachecorbula*. The shell although not smaller is much thinner than in
412 most corbulids and in this could be regarded as stunted. We propose that progenesis has
413 not occurred but the extreme conditions have stunted the growth of selected tissues and
414 organs. The large ctenidium is retained in order to maximise food particle collectionand

415 respiration, and the thin shell can reduce energy demand. The large, thin shell, which can
416 be regarded as a neotenous character, does not increase predation pressure as predators
417 are not abundant.
418
419 Colonisation of the shores of the brine pool is therefore negatively influenced by the
420 extreme environmental parameters but these are partly mitigated by biological parameters
421 such as lack of competition and few predators.
422
423 In the systematic section we noted that corbulids are infrequent in the bathyal and abyssal
424 regions of the deep oceans across the world. The Red Sea appears to be an exception with
425 species being recorded from the Thuwal seep at a depth of 840 – 850m (Batang et al,
426 2012) and the *C. (Varicorbula)* sp. 1 from 1465m (this paper). Such bathymetric range
427 extensions are not unusual for Red Sea invertebrates and it is argued that the high
428 temperatures maintained in the deep Red Sea allow shallow warm water taxa to exist at
429 greater depths (Turkay, 1996). High levels of endemism are recorded for the deep Red
430 Sea fauna (Turkay, 1996) and to date corbulids have not been recorded from depths
431 beyond the shelf in the adjacent Gulf of Aden and Arabian Seas. The deepest records are
432 those of *Corbula subquadrata* Melvill & Standen, 1907 and *C. persica* Smith 1906 from
433 285 m in the Gulf of Oman (Melvill & Standen, 1907).
434
435 Both *Apachecorbula* and *Corbula* sp. 1 can be added to the list of endemics from the Red
436 Sea. The various environmental crisis experienced by the Red Sea including periods of
437 hypersalinity and anoxia (Braithewaite, 1987) could have simulated current brine pool
438 conditions at shallow depths creating an adaptive force in the shallow water fauna.
439

440 ## ACKNOWLEDGEMENTS

441
442 We are grateful to all help from the other Leg 4 Red Sea Expedition 2013 KAUST
443 participants; Ioannis Georgakakis, Thor A. Klevjer, Perdana Karim Prihartato, Anders
444 Røstad and Ingrid Solberg. Leonidas Manousakis and Manolis Kalergis from Hellenic
445 Centre for Marine Research (HCMR) assisted in ROV operations. The captain and crew

of R/VAegaeo provided support during the entire cruise. Ohoud Mohammed Eid Alharbi assisted with the electron microscopy. The Red Sea Expedition 2013 was sponsored by KAUST.

REFERENCES

Allen J.A. (2008) Bivalvia of the Deep Atlantic. *Malacologia* 50(1–2), 57–173.

Allen J.A. (1979) The adaptations and radiation of Deep-sea bivalves. *Sarsia*. 64, 19-27.

Anderson L.C. and Roopnarine P.D. (2003) Evolution and phylogenetic relationships of Neogene Corbulidae (Bivalvia: Myoidea) of tropical America. *Journal of Paleontology* 77(6), 1086–1102.

Anisimova M., Gascuel O. (2006) Approximate likelihood ratio test for branchs: A fast, accurate and powerful alternative. *Systematic Biology* 55(4), 539-52.

Antunes A., Ngugi D.K. and Stingl U. (2011) Microbiology of the Red Sea (and other) deep-sea anoxic brine lakes. *Environmental Microbiology Reports* 3(4), 416–433.

Batang Z.B., Papathanassiou E., Al-Suwailem A., Smith C., Salomidi M., Petihakis G., Alikunhi N.M., Smith L., Mallon F., Yapici T. and Fayad N. (2012) First discovery of a cold seep on the continental margin of the central Red Sea. *Journal of Marine Systems* 94, 247–253.

Bischoff J.L. (1969) Red Sea geothermal brines deposits: their mineralogy, chemistry and genesis. In Degens D.T. and Ross D.A. (Eds.) *Hot brines and Recent Heavy Metal Deposits in the Red Sea.* Springler Verlag, New York, pp. 308–401.

Braithwate C.J.R. (1987) Geology and paleogeography of the Red Sea region. In Edwards A.J. and Head S.M. (Eds) *Key environments. Red Sea*, Pergamon Press, Oxford, New York pp. 22-44.

Brown R.W (1956) *Composition of Scientific Words*. Smithsonian Institution Press, London and Washington, 882 pp.

Carney S.L., **Formica M.I.**, **Divatia H.**, **Nelson K.**, **Fisher C.R.**, **Schaeffer S.W**. (2006) Population structure of the mussel "*Bathymodiolus*" *childressi* from Gulf of Mexico hydrocarbon seeps. *Deep Sea Research Part I*. 53 (6), 1061–1072 http://dx.doi.org/10.1016/j.dsr.2006.03.002

Castresana J. (2000) Selection of conserved blocks from multiple alignments for their use in phylogenetic analysis. *Molecular Biology and Evolution* 17(4), 540-52.

Chevenet F., Brun C., Banuls A.L., Jacq B., Chisten R. (2006) TreeDyn: towards dynamic graphics and annotations for analyses of trees. *BMC Bioinformatics* 10;7:439.

Cordes E.E., Hourdez S., Roberts H.H. (2010) Unusual habitats and organisms associated with the cold seeps of the Gulf of Mexico. In: Kiel S (ed) *The Vent and Seep Biota. Topics in Geobiology* pp. 315-332.

Dereeper A., Guignon V., Blanc G., Audic S., Buffet S., Chevenet F., Dufayard J.F., Guindon S., Lefort V., Lescot M., Claverie J.M., Gascuel O. (2008) Phylogeny.fr: robust phylogenetic analysis for the non-specialist. *Nucleic Acids Research* 1;36

Edgar R.C. (2004) MUSCLE: multiple sequence alignment with high accuracy and high throughput. *Nucleic Acids Research* 19;32(5),1792-7.

Folmer, O., Black, M., Hoeh, W., Lutz, R. and Vrijenhoek, R. (1994) DNA primers for amplification of mitochondrial cytochrome c oxidase subunit I form diverse metazoan invertebrates. *Molecular Marine Biology and Biotechnology* 3, 294–299.

Giribet, G., Carranza, S., Baguñà, J., Riutort, M. and Ribera, C. (1996) First molecular evidence for the existence of a Tardigrada + Arthropoda clade. *Molecular Biology and Evolution* 13, 76–84.

Grill B. and Zuschin M. (2001) Modern shallow- to deep-water bivalve death assemblages in the Red Sea ecology and biogeography. *Palaeogeography, Palaeoclimatology, Palaeoecology* 168, 75-96

Guindon S., Gascuel O. (2003) A simple, fast, and accurate algorithm to estimate large phylogenies by maximum likelihood. *Systematic Biology* 52(5), 696-704.

Gustafson R.G., Turner R.D., Lutz R.A. and Vrijenhoek R.C. (1998) A new genus and five new species of mussels (Bivalvia: Mytilidae) from deep-sea sulfide/hydrocarbon seeps in the Gulf of Mexico. *Malacologia* 40(1-2), 63-112.

Hallan A., Colgan D.J., Anderson L.C., García A and Chivas A.R.A. (2013) A single origin for the limnetic–euryhaline taxa in the Corbulidae (Bivalvia). *Zoologica Scripta* 42(3), 278-287.

Hartmann M. (1985) Atlantis II deep geothermal brine system. Chemical processes between hydrothermal brines and Red Sea deep water. *Marine Geology* 64, 157–177.

Hayami, I. and Kase, T. (1993) Submarine cave bivalvia from the Ryukyu Islands: systematics and evolutionary significance. *The University Museum, The University of Tokyo, Bulletin* 35, 1–133.

Lampadariou N., Hatziyanni E. and Tselepides A. (2003) Community structure of meiofauna and macrofauna in Mediterranean deep-hyper-saline anoxic basins: CIESM, 2003. *Mare Incognitum? Exploring Mediterranean deep-sea biology.* CIESM Workshop Monographs n°23, 128 pages, Monaco www.ciesm.org/publications/Heraklion03.pdf

Lorion, J., Buge, B., Cruaud, C. and Samadi, S., (2010) New insights into diversity and evolution of deep-sea Mytilidae (Mollusca: Bivalvia). *Molecular Phylogenetics and Evolution* 57, 71–83.

MacDonald I.R., Guinasso H.L., Reilly Brooks J.M., Callender W.R. and Gabrielle S.G. (1990) Gulf of Mexico hydrocarbon seep communities. VI. Patterns in community structure and habitat. *Geo-Marine Letters* 10, 244–252.

Melvill J.C. and Standen R. (1907) The Mollusca of the Persian Gulf, Gulf of Oman and Arabian Sea, as evidenced mainly through the collections of Mr. F. W. Townsend, 1893-1906; with descriptions of new species. Part II.- Pelecypoda. *Proceedings of the Zoological Society of London* 1906, 783-848.

Mikkelsen P.M. and Bieler R. (2001) *Varicorbula* (Bivalvia: Corbulidae) of the western Atlantic: taxonomy, anatomy, life habits, and distribution. *The Veliger* 44, 271–293.

Morton B. (1990) The biology and functional moorpholgy of *Corbula crassa* (Bivalvia: Corbulidae) with special reference to shell structure and formation. In B. Morton (ed.) *The Marine Flora and Fauna of Hong Kong and Southern China II. Volume 3. Behaviour, Morphology, Physiology and Pollution.* Hong Kong University Press, Hong Kong, pp. 1055–1073.

Ockelmann K.W. (1964) *Turtonia minuta* (Fabricius), A neotenous veneracean bivalve. *Ophelia* 1(1), 121-146.

Oliver P.G. (1979) Adaptations of some deep-sea suspension feeding bivalves (*Limopsis*

and *Bathyarca*) *Sarsia* 64, 33-36.

Oliver P.G. (2001) Functional morphology and description of a new species of *Amygdalum* (Mytiloidea) from the oxygen minimum zone of the Arabian Sea. *Journal of Molluscan Studies* 67, 225-241.

Salas C. (1994) *Notolimea clandestina* a new species of neotenous bivalve (Bivalvia: Limidae) endemic to the Strait of Gibraltar. *Journal of Molluscan Studies*. 63(3), 249-254.

Taylor J.D. and Glover E.A. (2010) Chemosymbiotic bivalves. In Kiel S (ed) *The Vent and Seep Biota. Topics in Geobiology*, pp 107-135.

Türkey M. (1996) Composition of the deep Red Sea macro- and megabenthic invertebrate fauna. Zoogeographie and ecological implications. In Uiblein F., Ott J. and Stachowitsch M. (Eds), *Deep-sea and extreme shallow-water habitats: affinities and adaptations. Biosystematics and Ecology*. Series 11, 43-59.

Whiting, M.F., Carpenter, J.C., Wheeler, Q.D., Wheeler, W.C. (1997) The Strepsiptera problem: Phylogeny of the holometabolous insect orders inferred from 18S and 28S ribosomal DNA sequences and morphology. *Systematic Biology* 46, 1–68.

Xiong, B. and Kocher, T.D., (1991) Comparison of mitochondrial DNA sequences of seven morphospecies of black flies (Diptera: Simuliidae). *Genome* 34, 306–311.

Yonge C.M. (1946) On the habits and adaptations of *Aloidis (Corbula) gibba*. *Journal of the Marine Biological Association of the United Kingdom* 26(3), 358-376.

Zierenberg R.A. and Shanks, III W.C. (1986) Isotopic constraints on the origin of the Atlantis II, Suakin and Valdivia brines, Red Sea. *Geochimica et Cosmochimica Acta*. 50, 2205-2214.

FIGURE LEGENDS

Fig. 1. Distribution of the major brine pools in the Red Sea.

Fig. 2. Chart of salinity, dissolved oxygen, pH and temperature with increasing depth in proximity to the Valdivia brine pool.

Fig. 3. Sea floor images at the margins of the Valdivia brine pool taken by the ROV Max Rover. *Apachecorbula* appear as black coloured clams in (A) and as small black objects arranged in a narrow band in (C). (B) shows the collecting bag of the ROV.

Fig. 4. Diagram showing the shell measurements used in the description.

Fig. 5. Shells of *Apachecorbula muriatica* gen et sp nov. (A-D): Holotype, NMW.Z. 2013.058.1. (E-H): Variations in outline and tumidity.

Fig. 6. Scanning electron micrographs of the shell of *Apachecorbula muriatica*. (A) left valve hinge; (B) dorsal view of left valve hinge; (C) right valve hinge; (D) weak serrations on the posterior flange of the right valve; (E) microsculpture on the umbonal area of the left valve; (F) radial creases in the periostracum at the margins of the left valve; (G) commarginal ridges at the margins of the right valve; (H) radial impressions on the shell after removal of the periostracum; Small spines on the dorsal margin of the early shell.

Fig. 7. Scanning electron micrographs of the shell of *Apachecorbula muriatica*. (A) cross section of the shell; (B, C) black surface coating showing structure as an accumulation of reticulate spherules.

Fig. 8. Gross anatomy of *Apachecorbula muriatica*. after dissection from the left side and stained in haematoxylin. (A) semi-diagrammatic reconstruction of the gross anatomy; (B) whole animal after removal of left valve and mantle; (C) siphonal openings; (D) visceral mass; (E) visceral mass with digestive gland and epithelium dissected away.

Fig. 9. Scanning electron micrographs of the ctenidium of *Apachecorbula muriatica*. (A) frontal surface; (B) abfrontal surface; (C) lateral frontal cirri and lateral cilia; (D) ciliation at the ventral edge of the inner demibranch.

Fig. 10. Shells of comparative species recorded from the Red Sea. (A, B), *Corbula (Varicorbula) erythraeensis;* (C, F), *C. (V.) rotalis*; (D,E), *C. (Anisocorbula) sulculosa*; (G, H), *C. (A.) taitensis*.

Fig. 11(A-D): Shells of *Corbula (Varicorbula)* sp. 1 Central Red Sea. E-F. *Apachecorbula muriatica*, large specimen for comparison.

Fig. 12. Scanning electron micrographs of juvenile shells of corbulid species. (A-B) *C. (V.) erythraeensis*, (A) whole left valve; (B) pustules on anterior slope. (C,D), *C. (A.) sulculosa* (A) whole left valve; (D) posterior carina and radial rows of pustules. (E) Internal of right valve of *C. (V.) gibba* showing dorsal spines. (F-I): *A. (V.)* sp. 1 (F) whole left valve; (G) umbonal region of right valve; (H) hinge of left valve; (I) hinge of right valve.

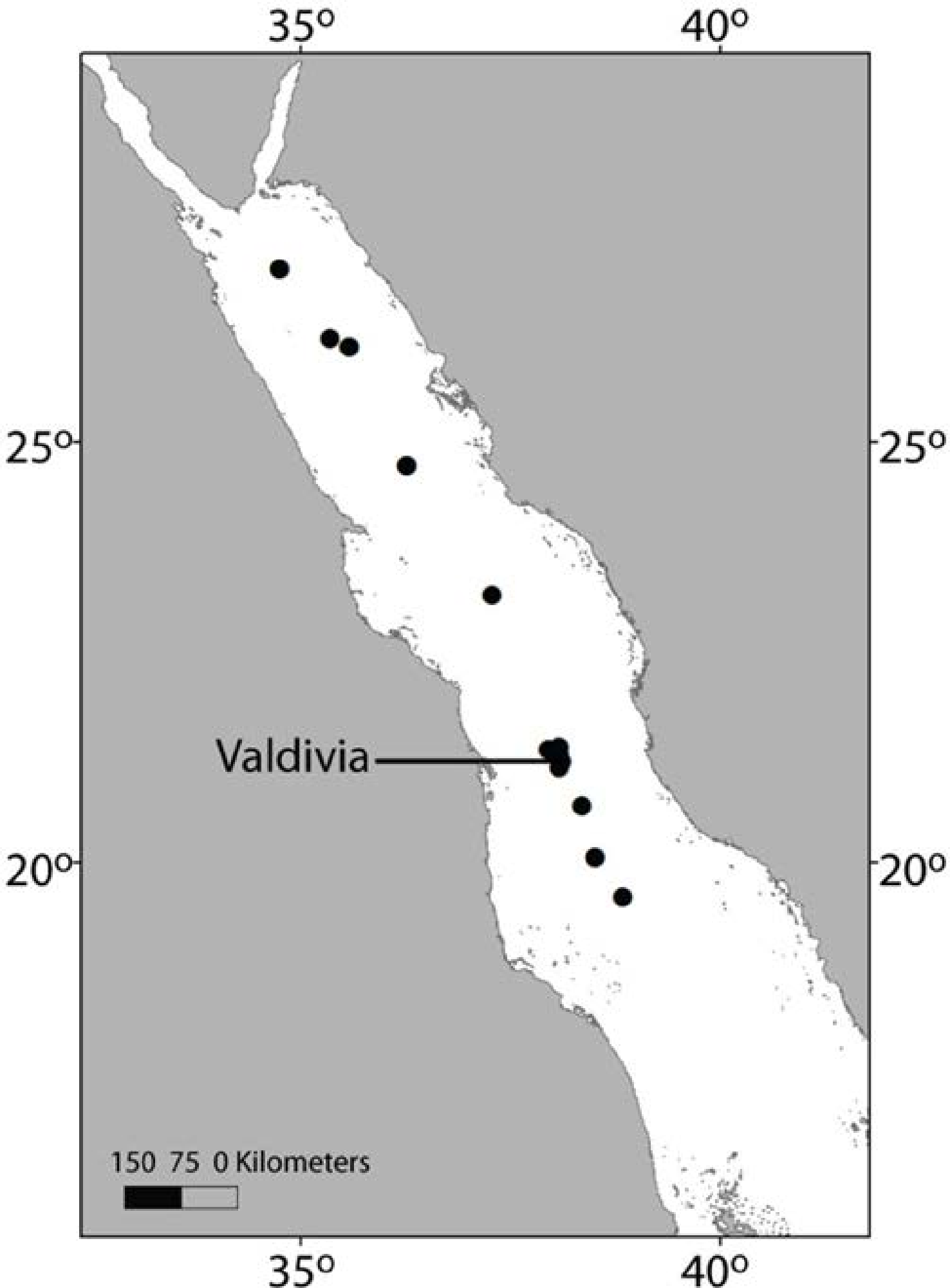
35°
40°
25°
25°
Valdivia
20°
20°
150 75 0 Kilometers
35°
40°

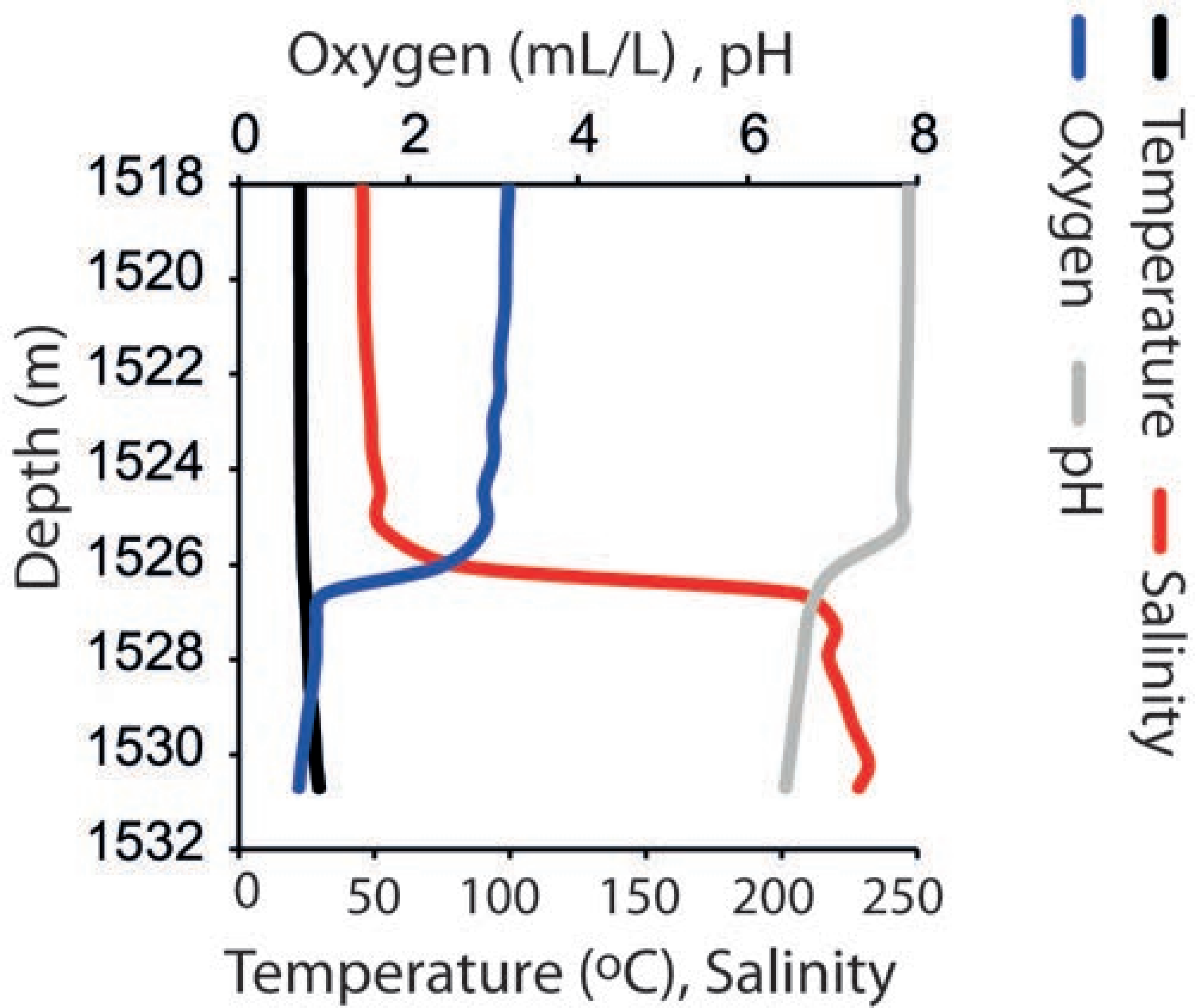
Oxygen (mL/L) , pH
0
2
4
6
8
1518
1520
1522
1524
1526
1528
1530
1532
Depth (m)
0
50
100
150
200
250
Temperature (ºC), Salinity
Oxygen
pH
Temperature
Salinity

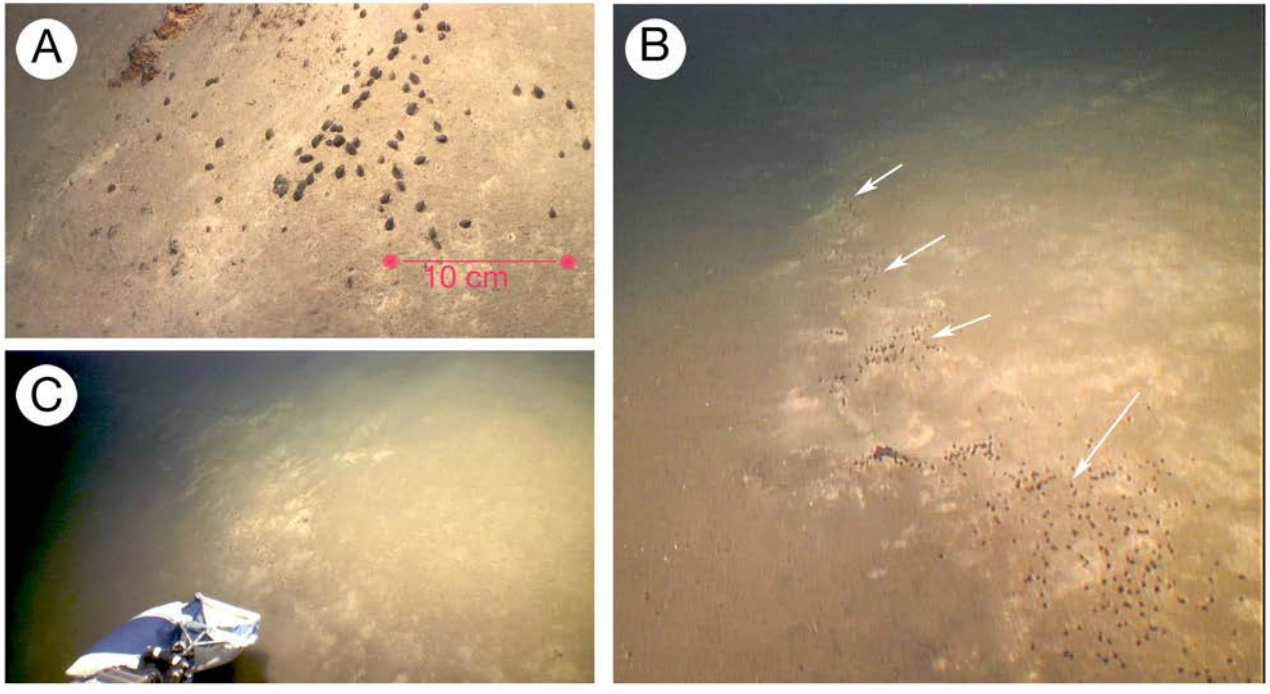
A
10 cm
B
C

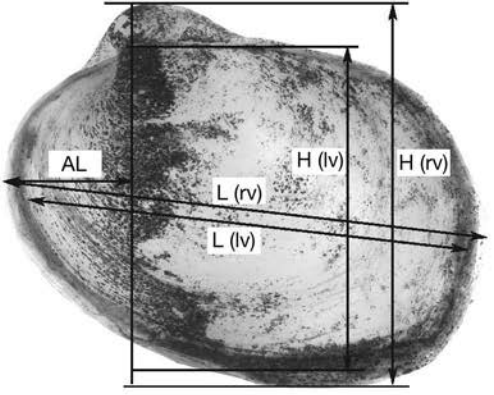
AL
H (lv)
H (rv)
L (rv)
L (lv)

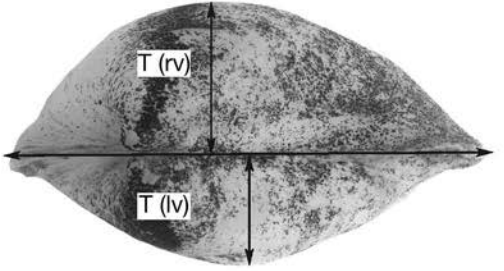
T (rv)
T (lv)

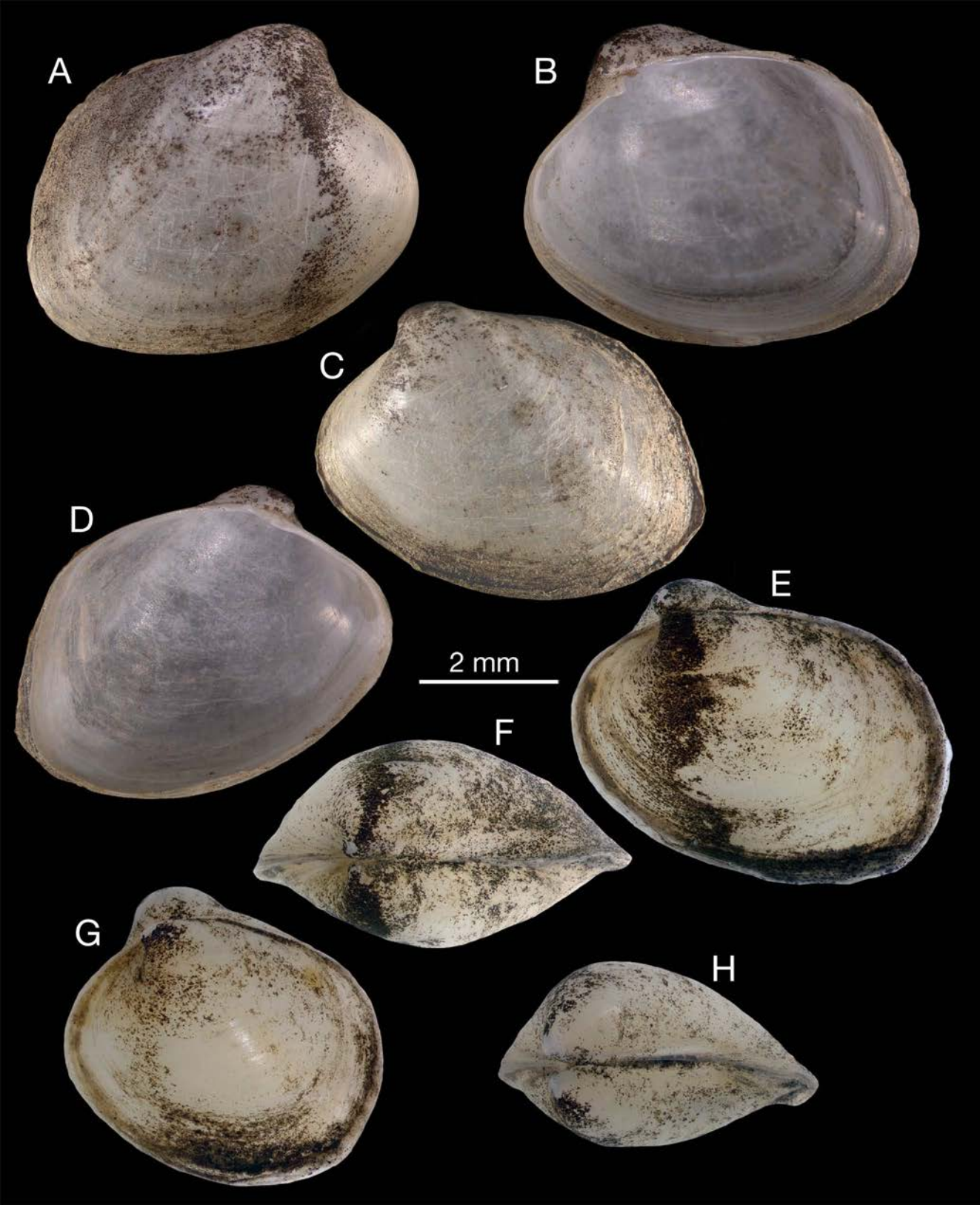
A
B
C
D
E
2 mm
F
G
H

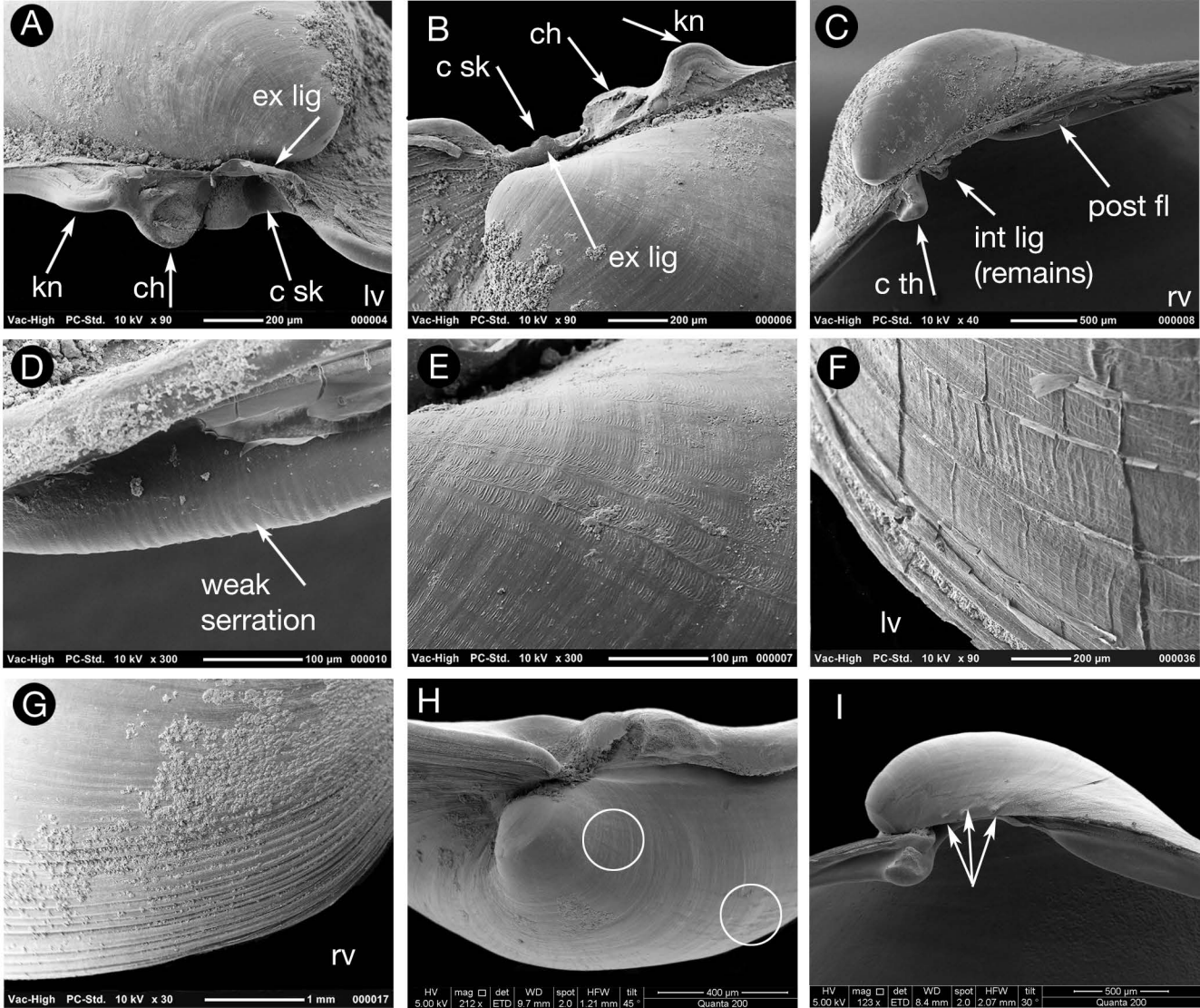
A
ex lig
kn
ch
c sk
lv
Vac-High PC-Std. 10 kV x 90 200 µm 000004
B
ch
kn
c sk
ex lig
Vac-High PC-Std. 10 kV x 90 200 µm 000006
C
post fl
int lig
(remains)
c th
rv
Vac-High PC-Std. 10 kV x 40 500 µm 000008
D
weak
serration
Vac-High PC-Std. 10 kV x 300 100 µm 000010
E
Vac-High PC-Std. 10 kV x 300 100 µm 000007
F
lv
Vac-High PC-Std. 10 kV x 90 200 µm 000036
G
rv
Vac-High PC-Std. 10 kV x 30 1 mm 000017
H
HV 5.00 kV | mag 212 x | det ETD | WD 9.7 mm | spot 2.0 | HFW 1.21 mm | tilt 45 ° | 400 µm | Quanta 200
I
HV 5.00 kV | mag 123 x | det ETD | WD 8.4 mm | spot 2.0 | HFW 2.07 mm | tilt 30 ° | 500 µm | Quanta 200

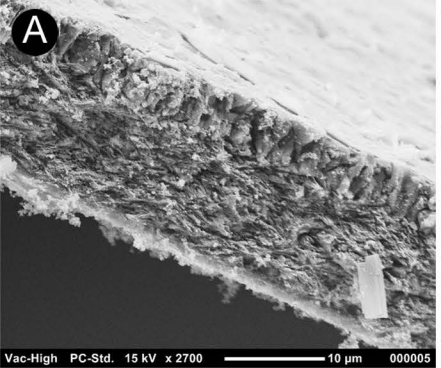
A
Vac-High PC-Std. 15 kV x 2700 10 µm 000005

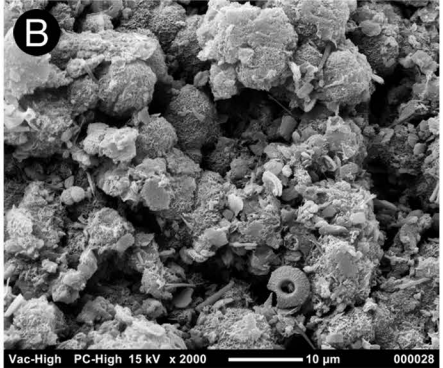
B
Vac-High PC-High 15 kV x 2000 10 µm 000028

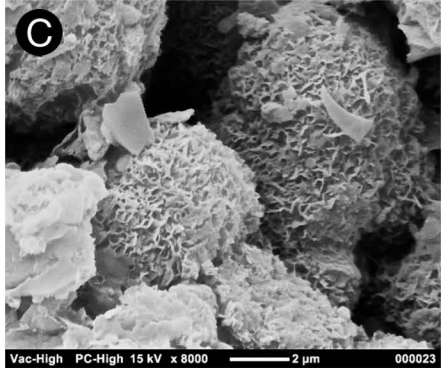
C
Vac-High PC-High 15 kV x 8000 2 µm 000023

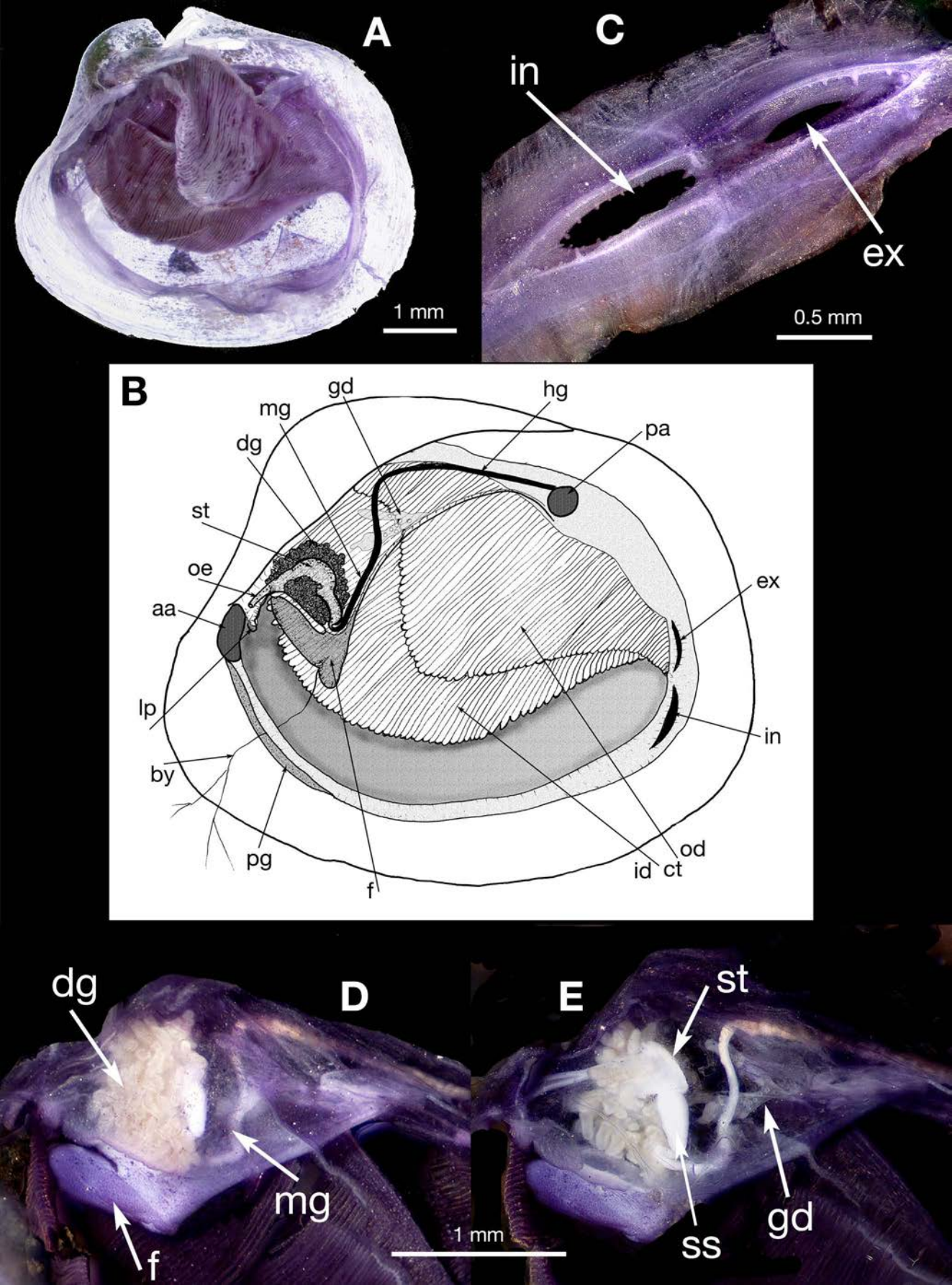
A
1 mm
C
in
ex
0.5 mm
B
gd
hg
mg
pa
dg
st
oe
ex
aa
lp
in
by
pg
od
id
ct
f
dg
D
mg
f
1 mm
E
st
ss
gd

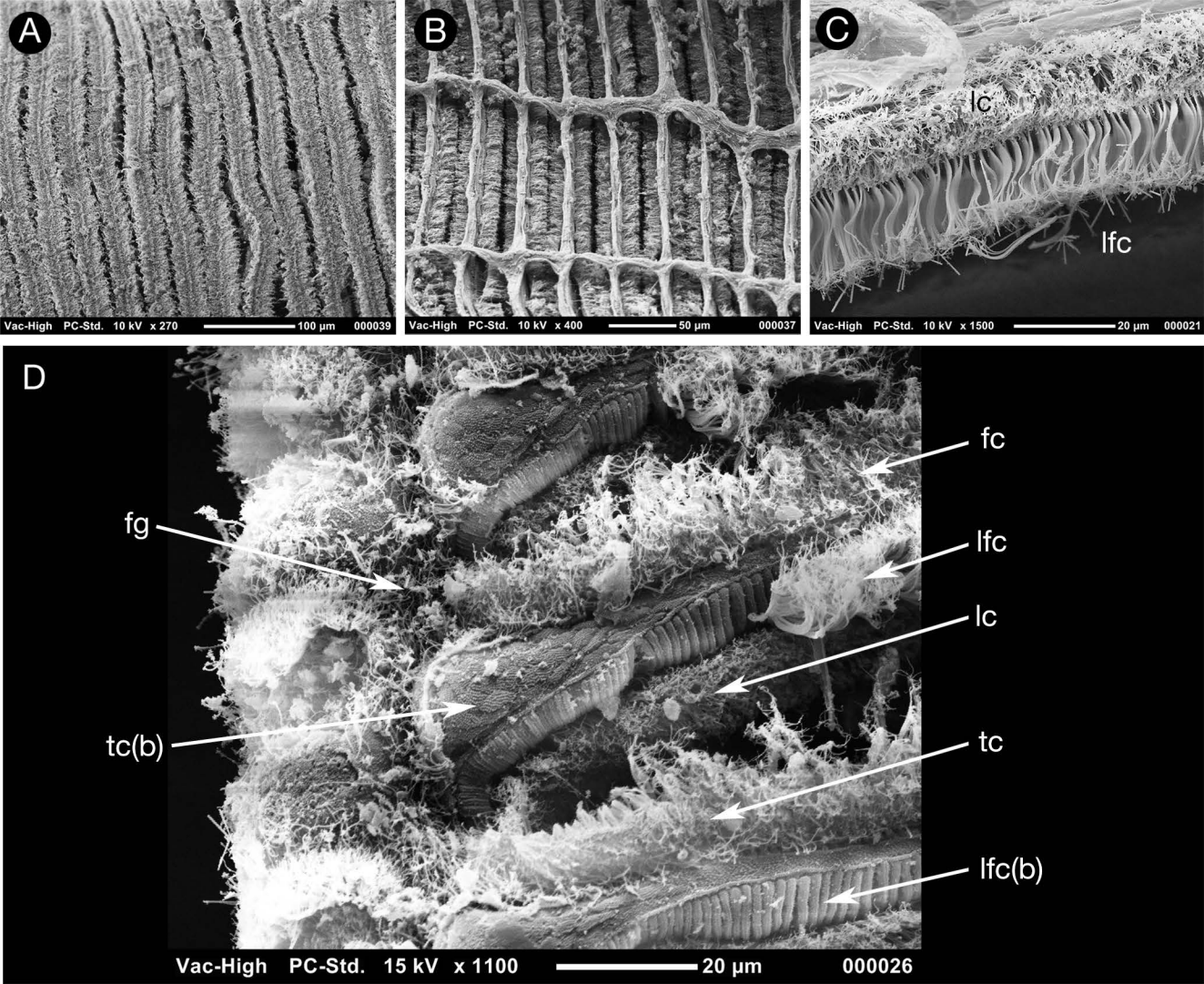
A
Vac-High PC-Std. 10 kV x 270 100 µm 000039
B
Vac-High PC-Std. 10 kV x 400 50 µm 000037
C
lc
lfc
Vac-High PC-Std. 10 kV x 1500 20 µm 000021
D
fg
fc
lfc
lc
tc(b)
tc
lfc(b)
Vac-High PC-Std. 15 kV x 1100 20 µm 000026

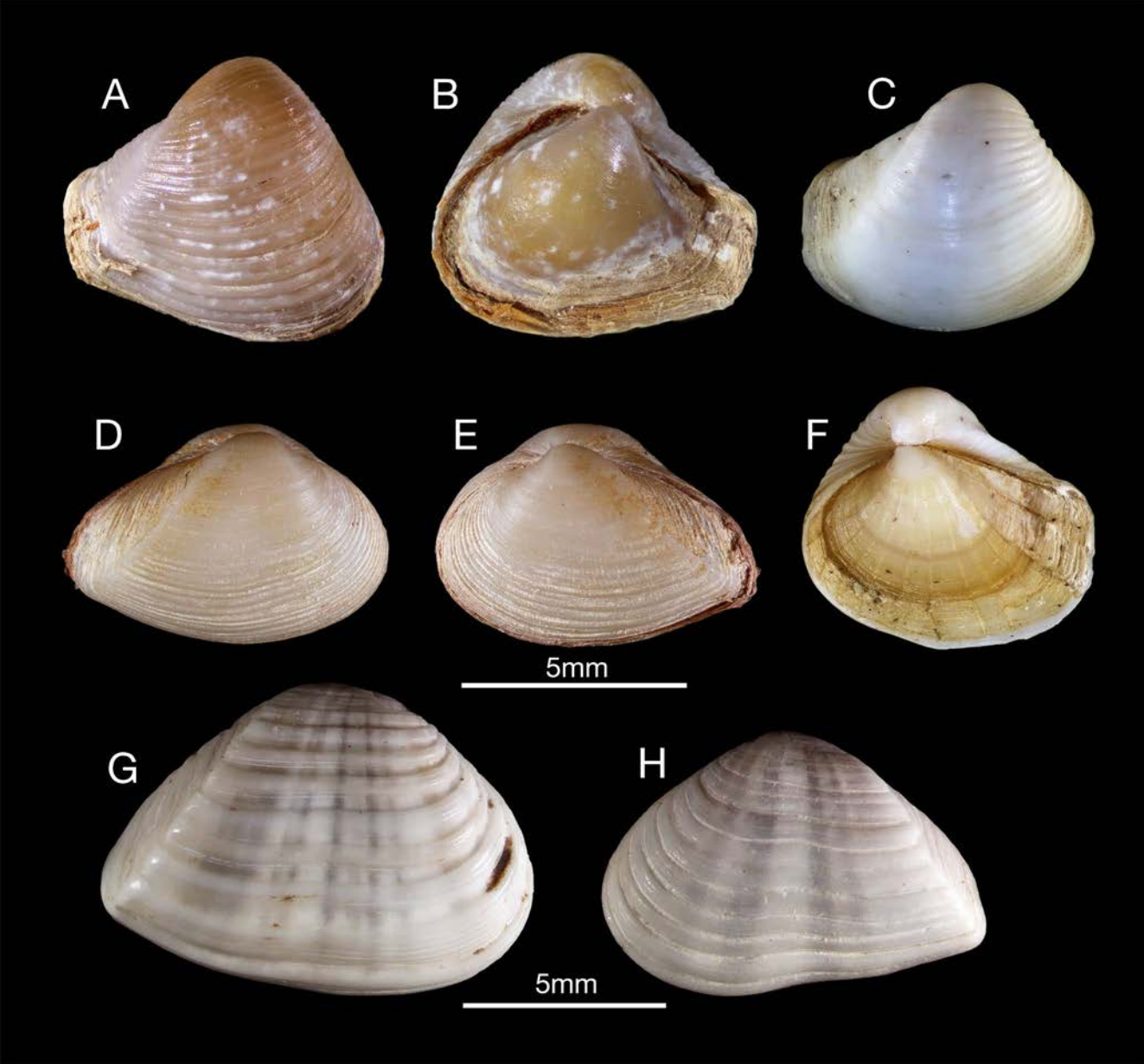
A
B
C
D
E
F
5mm
G
H
5mm

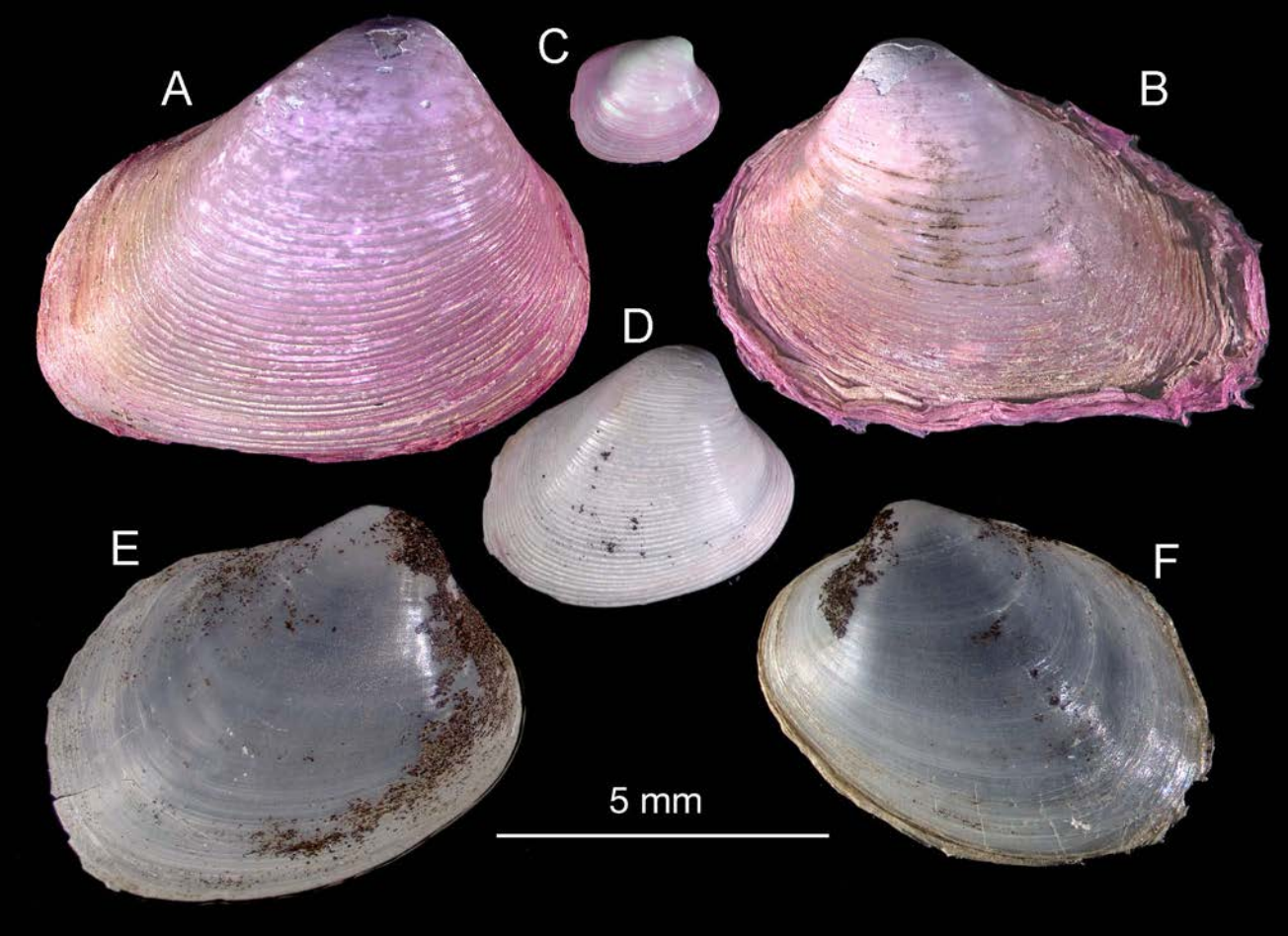
A
C
B
D
E
F
5 mm

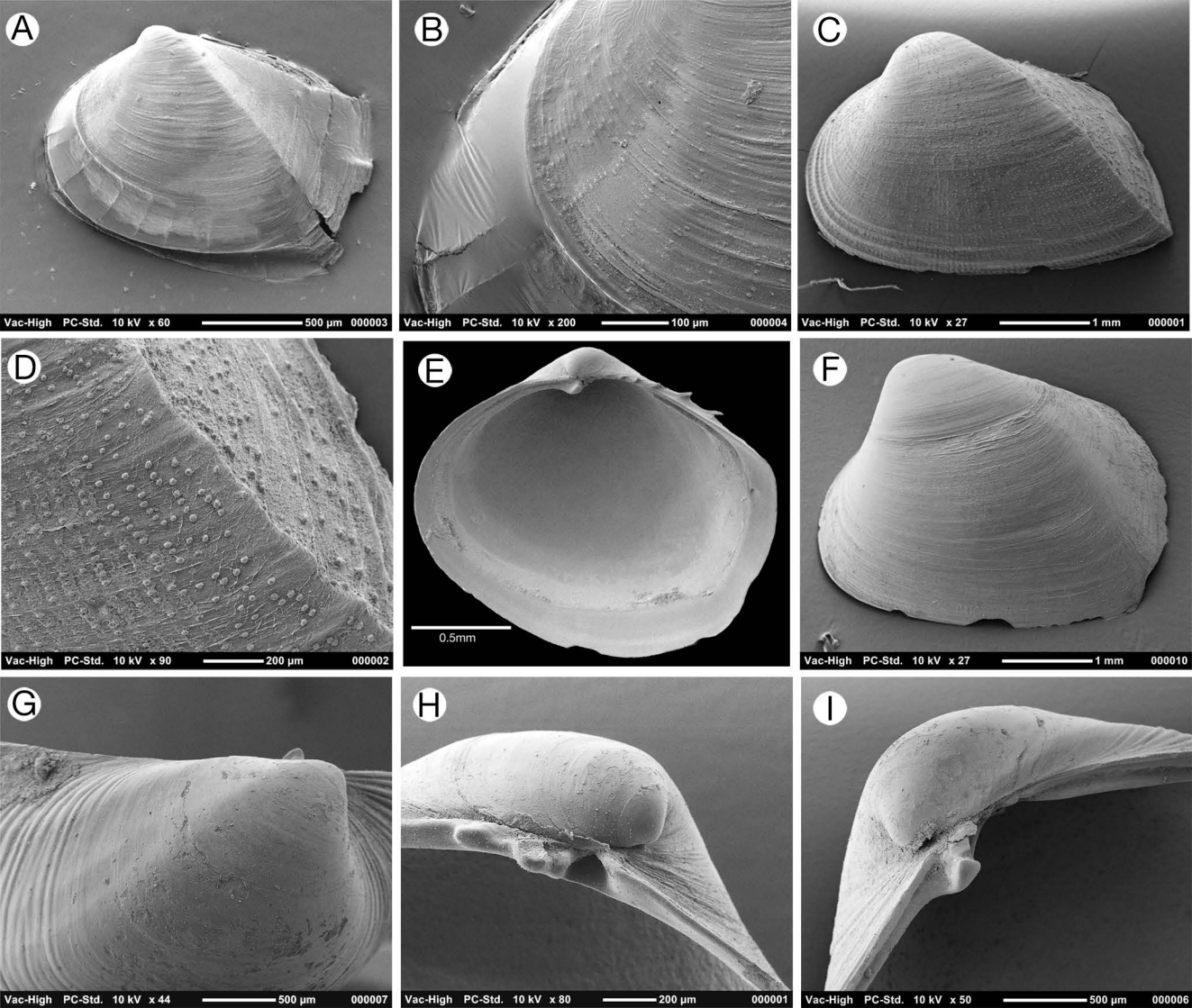
A
Vac-High PC-Std. 10 kV x 60 500 µm 000003
B
Vac-High PC-Std. 10 kV x 200 100 µm 000004
C
Vac-High PC-Std. 10 kV x 27 1 mm 000001
D
Vac-High PC-Std. 10 kV x 90 200 µm 000002
E
0.5mm
F
Vac-High PC-Std. 10 kV x 27 1 mm 000010
G
Vac-High PC-Std. 10 kV x 44 500 µm 000007
H
Vac-High PC-Std. 10 kV x 80 200 µm 000001
I
Vac-High PC-Std. 10 kV x 50 500 µm 000006